Probing the Binding of Propranolol Enantiomers to α_1-Acid Glycoprotein with Ligand-Detected NMR Experiments

Bridget A. Becker[†] **and Cynthia K. Larive***

Department of Chemistry, University of California, Riverside, Riverside, California 92521

Received: July 8, 2008; Revised Manuscript Received: August 23, 2008

Mapping the interactions of a small molecule ligand with a protein can provide information important for biochemical studies and for drug design and development. This information can be determined using the ligand-detected ^{1}H NMR experiments $T_{1\rho}$-NOESY, diffusion, and saturation transfer difference (STD). This work compares the results of these experiments and examines their ability to distinguish the binding epitopes of propranolol enantiomers with α_1-acid glycoprotein (AGP). The epitope maps for the propranolol enantiomers are fairly similar, as expected from their similar binding affinities; however, the STD epitope maps provide unique insights into the different orientations of the enantiomers with respect to the AGP binding pocket. Our results suggest that it is best to consider the data provided by several NMR epitope mapping experiments in drawing conclusions about ligand−protein binding interactions.

Introduction

This study investigates the use of the ligand-detected ^{1}H NMR experiments to study the binding of the *R* and *S* enantiomers of propranolol, a chiral β-adrenergic receptor antagonist, with the human serum protein α_1-acid glycoprotein (AGP), also known as orosomucoid. AGP is the primary transporter for basic drugs in the blood.[1,2] Understanding the nature of interactions of potential drug compounds and plasma proteins such as human serum albumin and AGP is important because protein binding significantly affects *in vivo* pharmacokinetics.[3−7] Chromatographic studies have provided important insights into drug−AGP interactions,[2,8−10] although some information has also been supplied by infrared, fluorescence, and circular dichroism studies.[6,11−15] The AGP binding site is thought to be a floppy, cone-shaped hydrophobic pocket containing a hydrophilic patch of negative charge, or hydrogen bond donors or acceptors near the apex. The hydrophobic portion of the binding site can accommodate many different sizes and shapes of hydrophobic moieties, while the specificity for basic drugs is conferred by interactions with the hydrophilic patch.[2,9] Fluorescence spectroscopy studies have implicated interactions with an AGP tryptophan residue and have suggested that the binding of progesterone does not alter the protein's structure.[15]

Although discovered in 1950, there is still no high-resolution structure of AGP.[16,17] AGP is extensively glycosylated with about 45% of the 41−43 kDa mass of AGP comprised of carbohydrate.[4,11] The carbohydrate moieties of AGP consist of five N-linked glycans with a high degree of sialylation accounting for the very low pI of this protein. Changes in the glycation of AGP have been shown to be important in its role in acute and chronic inflammation.[18] Because of its extensive glycosylation, it is difficult to obtain crystals of suitable quality for high-resolution X-ray crystallography or to express isotopically labeled glycosylated AGP for NMR structural studies. Therefore, ligand-detected NMR experiments are ideal to probe the nature of propranolol−AGP binding.[19] The goal of this work is to critically compare the results obtained for the binding of the propranolol enantiomers to AGP using the ligand-detected nuclear Overhauser effect spectroscopy (NOESY), diffusion, and saturation transfer difference (STD) experiments. To our knowledge, this is the first attempt to use ligand-detected NMR experiments to distinguish ligand−protein interactions based solely on chirality.

Experimental Methods

Materials. (*R*)-Propranolol (Tocris, Bristol, U.K.), (*S*)-propranolol (Biomol Research Laboratories, Plymouth Meeting, PA), human AGP (Sigma, Saint Louis, MO), and D_2O (Cambridge Isotope Laboratories, Andover, MA) were used as received. Commercial AGP is prepared from pooled serum and is therefore a mixture of protein sequence variants and glycosylation isoforms.[6,20] Solid sodium phosphate monobasic and sodium phosphate dibasic are from Fisher Scientific, Fair Lawn, NJ. To reduce the HOD signal from the buffer, solutions of monobasic and dibasic phosphate dissolved in D_2O were lyophilized and reconstituted in D_2O. The pH of all propranolol/AGP solutions was maintained at pD 7.46 using a 50 mM sodium phosphate buffer. Solutions of different concentration ratios of propranolol and AGP were prepared by combining aliquots of a buffered 0.1 mM AGP solution and a buffered solution containing 0.1 mM AGP and 20 mM propranolol, thereby maintaining a constant AGP concentration as the concentration of propranolol was varied.

NMR Experiments. All NMR spectra were acquired with a Bruker Avance 600 MHz NMR spectrometer with a broadband inverse probe equipped with *x*, *y*, and *z* gradients. The $T_{1\rho}$-filtered NOESY experiment was phase cycled, as described by Scherf and Anglister.[21] Each of the 512 increments was signal averaged for 64 scans and collected over 2048 complex points with a 2 s relaxation delay. The spectra shown are at a mixing time of 600 ms with a 20 ms spin-lock at a power level of 13 dB. Although the $T_{1\rho}$-filter length was optimized to 20 ms, many protein resonances remain, especially in the carbohydrate region between 3 and 4.5 ppm. A NOESY mixing time of 600 ms was selected for these experiments because it yielded a good signal-to-noise ratio for the intermolecular cross peaks. The

* Corresponding author. E-mail: clarive@ucr.edu.
[†] Current address: Merck Research Laboratories, 33 Avenue Louis Pasteur, Boston, MA 02115.

10.1021/jp8060366 CCC: $40.75
Published on Web 10/08/2008

Fourier transformation was performed on 2048 points in each dimension, with zero filling in F1 to 2048 points. Both dimensions were apodized by multiplication by a 90° shifted sine bell squared function.

BPPSTE diffusion experiments for both the protein−ligand and protein only solutions were acquired with the same parameters to facilitate spectral subtraction. Each of 16 experiments in which the gradient amplitude was varied from 3.32 to 19.89 G/cm was signal averaged for 1024 scans over 18026 complex points. The diffusion period, during which magnetization exchange occurs by NOE, was 600 ms. Gradient pulses of 1 ms duration were followed by a 100 μs delay to reduce the effect of eddy currents. A 1 ms homospoil pulse was applied during the diffusion delay to eliminate residual transverse magnetization. Each spectrum was zero filled to 65 536 points and multiplied by an exponential function equivalent to 2 Hz line broadening prior to subtraction of the protein spectrum from the protein−ligand spectrum.

For all solutions other than 1 mM propranolol and 0.1 mM AGP, the on- and off-resonance STD spectra were measured by coadding 512 scans preceded by 16 dummy scans. For the solution of 1 mM propranolol and 0.1 mM AGP, it was necessary to coadd 2048 scans preceded by 16 dummy scans to yield detectable signals in the subtracted spectrum. In STD experiments, to examine buildup and select the optimum saturation time for epitope mapping, the repetition time was held constant at 4 s as the saturation time was varied. On the basis of the buildup curves, a saturation time of 1 s was chosen for the epitope mapping experiments. A train of 50 ms Gaussian-shaped pulses were used to comprise the total saturation time (20 pulses for 1 s saturation) at a power level of 62.28 dB. A 50 ms spin-lock at a power level of 13 dB was applied to suppress the protein background. A 3 ms homospoil gradient pulse was applied at the beginning of the experiment to eliminate unwanted transverse magnetization. Line broadening of 2 Hz was applied to each spectrum to improve the signal-to-noise ratio of the subtracted spectra.

The inversion−recovery experiment was used to measure T_1 relaxation times of the propranolol protons (Supporting Information Table S1) in solutions containing 8 mM propranolol and 0.1 mM AGP with eight scans collected for each increment over 23 362 complex points. The T_1 relaxation times measured for (*R*)- and (*S*)-propranolol are very similar. The T_1 recovery delay was arrayed over 16 different values from 0.01 to 15 s. The relaxation delay was 15 s which was determined in a separate parameter optimization experiment to be greater than 5 times the longest T_1 relaxation time of the ligand protons. T_1 relaxation times were calculated using the T_1/T_2 relaxation module in the Bruker Topspin v 1.3 software.

Results

The structure of propranolol is shown in Figure 1 along with its ^{1}H NMR spectrum. The propranolol ^{1}H NMR chemical shifts in D_2O solution at pD 7.46 are reported in Table 1 relative to the internal reference trimethylsilylpropioniate-2,2,3,3,d_4 (0.00 ppm). The dissociation constants (K_d) for the propranolol enantiomers and AGP have been previously determined by ultrafiltration as 1.58 μM for (*S*)-propranolol and 2.65 μM for (*R*)-propranolol.[5]

Information about the extent to which different ligand functional groups interact with a target protein can reveal important insights about ligand recognition and can contribute to rational lead optimization in drug discovery.[22] This information can be gathered through a process known as epitope mapping using several ligand-detected NMR experiments, including NOESY,[21−24] diffusion,[3,25,26] and STD.[27−30]

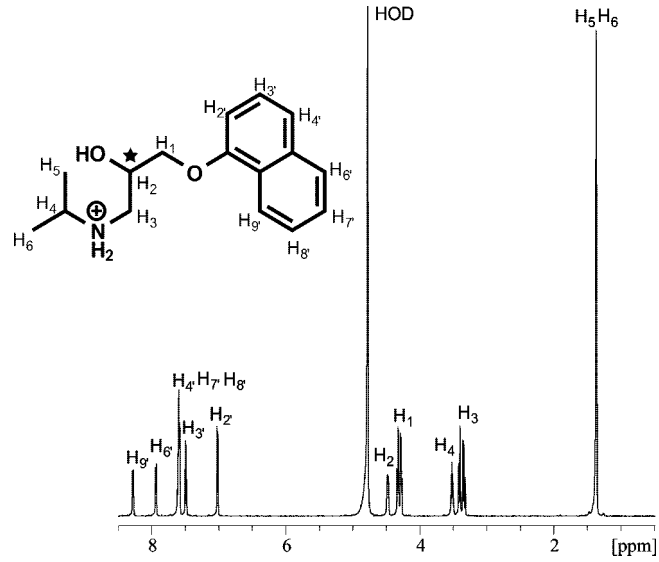

Figure 1. Structure of propranolol and the propranolol proton spectrum with the protons and corresponding resonances labeled.

TABLE 1: Propranolol ^{1}H NMR Chemical Shifts, κ Values, and Epitope Maps Obtained from Diffusion Experiments (The Results for the H_4 Resonance Could Not Be Reliably Determined due to Overlap with the Residual Carbohydrate Resonances of AGP)

	protons	(*S*)-propranolol		(*R*)-propranolol	
propranolol	δ (ppm)	$\kappa \times 10^{12}$	%	$\kappa \times 10^{12}$	%
H_1	4.27	1.77	89	1.82	81
H_2	4.46	1.40	71	1.39	70
H_3	3.35	1.81	91	2.26	100
H_4	3.49	ND		ND	
H_5, H_6	1.34	1.56	79	1.76	78
$H_{2'}$	6.99	1.98	100	1.99	88
$H_{3'}$	7.46	1.76	89	1.93	85
$H_{4'}$, $H_{7'}$, $H_{8'}$	7.57	1.93	97	2.06	91
$H_{6'}$	7.91	1.92	97	1.96	87
$H_{9'}$	8.25	1.72	87	1.62	72

$T_{1\rho}$-Filtered NOESY. NOESY experiments for epitope mapping detect intermolecular ligand−protein NOEs. These experiments should not be confused with transferred NOE experiments in which intramolecular ligand cross peaks are analyzed to determine the bound ligand conformation or aid in drug design through protein-mediated ligand−ligand NOEs.[31−33] The $T_{1\rho}$-filtered version of the NOESY experiment was used in this work to reduce the intensity of intramolecular protein−protein cross peaks and allow the detection of intermolecular ligand−protein cross peaks.[21] A consequence of protein resonance suppression by the $T_{1\rho}$ filter is that intermolecular cross peaks are not expected to appear symmetrically with respect to the diagonal because they are detected only in the F2 dimension.

Because the $T_{1\rho}$-filtered NOESY spectra of solutions of 20 mM (*R*)- or (*S*)-propranolol with 0.1 mM AGP are very similar, only the spectrum of the (*S*)-enantiomer is shown in Figure 2A. A strong cross peak between the propranolol methyl resonance at 1.34 ppm and the AGP methyl resonances, highlighted in Figure 2A by an oval, suggests strong hydrophobic interactions between the ligand methyl protons and aliphatic residues within the AGP binding pocket. An additional set of broad intermolecular cross peaks is observed between the resonances of the

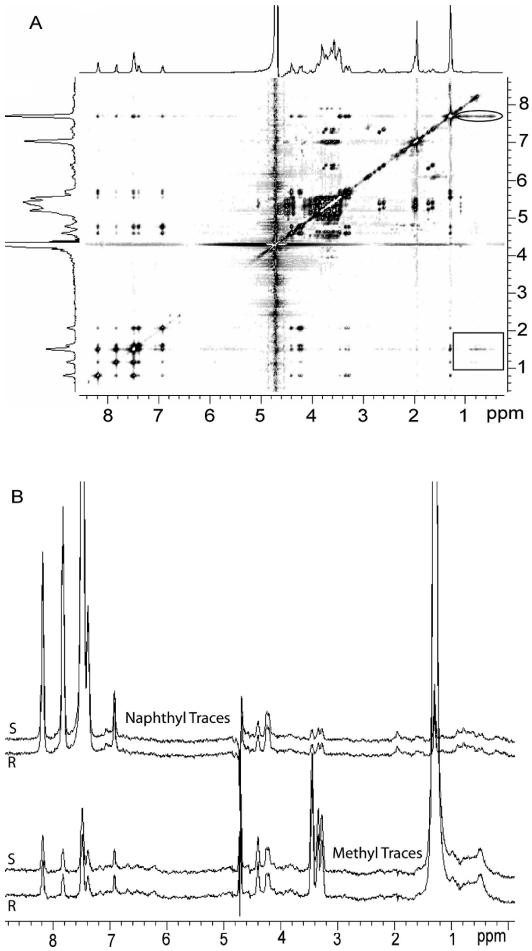

Figure 2. (A) $T_{1\rho}$-filtered NOESY spectrum of 2 mM (*S*)-propranolol and 0.1 mM AGP with F1 and F2 projections plotted on the left and top of the spectra, respectively. The oval indicates the cross peaks between AGP and the propranolol methyl resonance, and the box indicates the cross peaks between AGP and the propranolol naphthyl resonances. (B) Traces extracted from the $T_{1\rho}$-filtered NOESY spectra of 2 mM (*S*)-propranolol and 0.1 mM AGP, and 2 mM (*R*)-propranolol and 0.1 mM AGP, labeled S and R, respectively. Traces are through the propranolol methyl resonances and overlapped naphthyl resonances as labeled.

hydrophobic propranolol naphthyl ring (6.8−8.3 ppm) and the AGP methyl protons (0.5−1 ppm) highlighted by the box in Figure 2A. The strongest of the ligand cross peaks in this region are due to the overlapped naphthyl $H_{4'}$, $H_{7'}$, and $H_{8'}$ resonances probably because a greater number of protons comprises this peak. At a higher level of vertical scale, weaker cross peaks are observed between the naphthyl $H_{3'}$ and $H_{6'}$ resonances, each of which arises from a single proton, and the AGP methyl protons. Intermolecular cross peaks to the remaining naphthyl protons, $H_{2'}$ and $H_{9'}$, are extremely weak. The T_1 relaxation time of $H_{6'}$ is comparable to that of $H_{9'}$, so if these protons were equally close to the protein protons their cross peaks should be of approximately equal intensity. The T_1 relaxation time for $H_{2'}$ is the shortest of all the aromatic protons, and this may contribute to its weaker cross peak intensity. However, in spectra measured with shorter mixing times, $H_{2'}$ still gave rise to much weaker cross peaks with AGP. On the basis of these observations, it appears that $H_{2'}$ and $H_{9'}$ are more distant from the protein than the other propranolol naphthyl protons.

The traces in Figure 2B were extracted from the 2D NOESY spectra of (*R*)- and (*S*)-propranolol. In addition to the intermolecular ligand−protein cross peaks, sharper and more intense

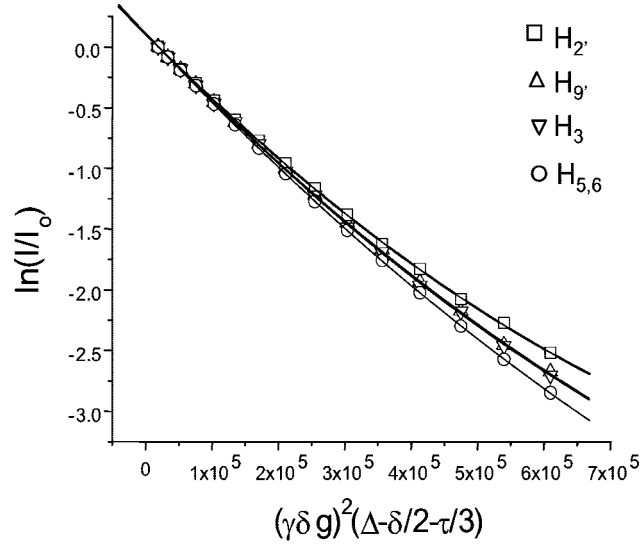

Figure 3. Selected diffusion decays for 4 mM (*S*)-propranolol and 0.1 mM AGP showing the differential curvature characteristic of magnetization exchange by NOE during the diffusion period.

intramolecular ligand NOEs are also observed. The intensity differences in the region 0−1.0 ppm in traces taken at the chemical shifts of the propranolol methyl resonances (bottom two traces labeled methyl traces in Figure 2B) or the overlapped naphthyl resonance of $H_{4'}$, $H_{7'}$, and $H_{8'}$ (top two traces labeled naphthyl traces Figure 2B) suggest that these ligand protons contact different aliphatic amino acid residues of AGP. The naphthyl traces in Figure 2B also show evidence of cross peaks between AGP aromatic resonances and the propranolol naphthyl group that are difficult to observe in the 2D plot. The observation of NOEs to the aromatic protons of AGP is consistent with fluorescence experiments that implicate a tryptophan residue in hydrophobic interactions with bound ligands.[14,15] Traces through other regions of the NOESY spectrum lacking these cross peaks showed no significant intensity, indicating that the cross peaks can be attributed to intermolecular NOEs and do not arise from baseline distortions or other artifacts.

Diffusion Measurements. In NMR diffusion experiments for epitope mapping, ligand resonance intensity is measured as a function of gradient amplitude for a fixed diffusion period. Because diffusion is a molecular property, in the absence of other effects, plotting the logarithm of resonance intensity versus the square of the gradient area should produce a straight line with a similar slope for each resonance of a molecule. However, when dipolar cross relaxation occurs during the diffusion period, intermolecular ligand−protein NOE is detected as different degrees of curvature in the linearized diffusion decays.[3,25,26] Although other mechanisms such as convection, temperature instability, or chemical exchange can cause equal curvature for all resonances, only NOE causes differential curvature among the diffusion decays for the various ligand protons. The diffusion decays shown in Figure 3 for a solution of 4 mM (*S*)-propranolol and 0.1 mM AGP were selected to show the range of curvature arising from magnetization exchange through NOE. The spectra used to produce the diffusion decays in Figure 3 were obtained by subtracting spectra measured for a propranolol−AGP solution and an identical solution containing only AGP at each gradient amplitude.[34] Table 1 shows the values of κ obtained by fitting a second-order polynomial to the measured diffusion decays along with the epitope maps calculated as percentages from these decays. There is not a great deal of difference in the magnitude of the κ values determined for the *R* and *S* enantiomers, with

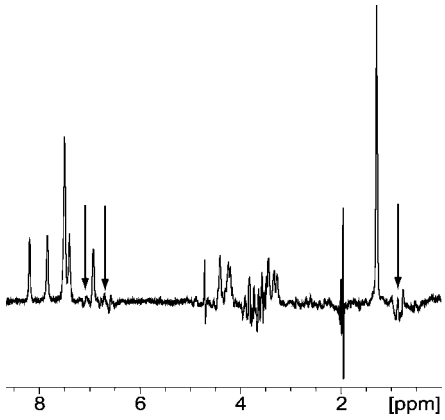

Figure 4. Spectrum extracted from a diffusion data set for 4 mM (*S*)-propranolol and 0.1 mM AGP. The arrows indicate subtraction artifacts due to changes in protein chemical shift resulting from ligand binding.

all κ values lying between 1.3 and 2.3 $\times$ 10^{-12}. Significant differences between the enantiomers are observed in the κ values for the methyl protons, H_3, and the overlapped resonance due to the naphthyl $H_{4'}$, $H_{7'}$, and $H_{8'}$. The eptiope maps in Table 1 are calculated by dividing each κ by the largest κ calculated in that experiment. Similar epitope maps are calculated for the two enantiomers. The diffusion results are consistent with close contact between AGP and the naphthyl ring and somewhat more distant contacts for the methyl groups. Unfortunately, subtraction artifacts in the region between 3 and 4 ppm of the diffusion spectra prevented quantification of the resonance intensity of H_4, which would provide important insights about contacts with the protonated amine.

Ligand resonances, especially at lower ligand:protein ratios, can be difficult to detect and quantify without reducing the broad spectral background produced by the protein. Because epitope mapping experiments rely on accurate measurements of ligand resonance intensity, protein resonance suppression is necessary to produce reliable ligand integrals. A typical diffusion spectrum produced by spectral subtraction is shown in Figure 4. Because the diffusion spectra used for subtraction were acquired in separate experiments for a propranolol−AGP solution and an identical solution of AGP alone, the subtraction artifacts are more severe than in experiments acquired in an interleaved format for the same solution, such as STD. Subtraction artifacts can result from temperature and magnetic field instability. This type of artifact is observed in the spectrum shown in Figure 4 in the region between 3 and 4 ppm and near 2 ppm.

Another type of subtraction artifact can be observed in Figure 4 in the methyl (0.5−1.0 ppm) and aromatic (6.5−7.5 ppm) regions of the spectrum. These artifacts arise because the protein resonances in the subtracted spectrum do not have the same chemical shift as the resonances in the solution containing both the protein and the ligand. Significant ring-current induced changes in chemical shift could be produced by close contact of the propranolol naphthyl ring and protons of protein binding pocket. Therefore, the artifacts highlighted by arrows in Figure 4 likely reflect changes in the chemical shift of hydrophobic amino acid residues affected by propranolol binding. The chemical shift of these subtraction artifacts closely matches the intermolecular ligand−protein NOEs observed in the $T_{1\rho}$-filtered NOESY results shown in Figure 2.

Saturation Transfer Difference. Typically, in STD experiments, the saturation frequency is chosen to irradiate the edge of the protein resonance envelop somewhere between 0 and −1 ppm and the effect of changing the saturation frequency is not interrogated. However, in experiments with AGP, saturation between 0 and −1 ppm was ineffective because the AGP spectrum does not have sufficient intensity in this region. Therefore, it was necessary to choose other saturation frequencies. Two irradiation frequencies, 0.33 and 2.6 ppm, were chosen to saturate the protein envelope while avoiding saturation of propranolol resonances.

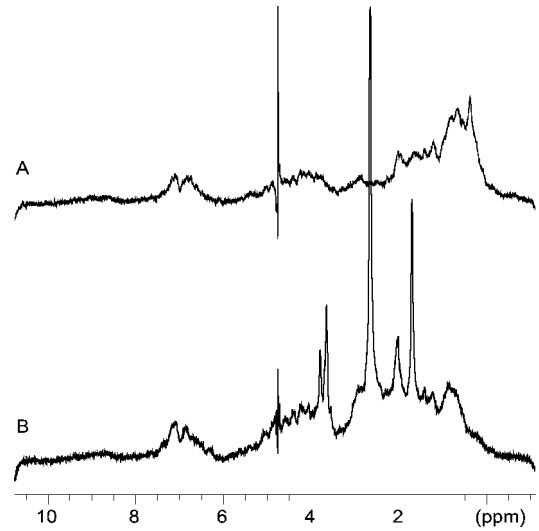

Figure 5. STD spectra for AGP alone showing differences in the spectra obtained with saturation at 0.33 ppm (A) and 2.6 ppm (B).

For many proteins, on-resonance saturation is efficiently transferred throughout the protein by spin diffusion; however, this is not the case for AGP. The STD spectra measured for a solution of only AGP with saturation at 0.33 and 2.6 ppm are shown in Figure 5. If saturation was spread evenly across the entire protein during the 1 s saturation time, the subtracted spectra shown in Figure 5 should perfectly overlay each other and would also be similar to the ^{1}H NMR spectrum of AGP. However, the spectrum in Figure 5A has greater intensity below 1.5 ppm compared with the spectrum in Figure 5B, which has more intensity in the region 1.5−3.5 ppm. Because saturation is not spread evenly throughout the protein, it will be transferred preferentially to those ligand protons interacting with the saturated protein protons. For example, STD experiments with the saturation frequency at 0.33 ppm should generate epitope maps that preferentially reflect propranolol interactions with the protein methyl protons, while saturation at 2.6 ppm should produce an epitope map that is more reflective of propranolol interactions with hydrophilic amino acid side chains, for example, aspartate and asparagine. Representative reference and STD spectra for a solution of (*R*)-propranolol and AGP with saturation at 0.33 ppm are shown in Figure 6.

The amount of time saturation is applied must be also optimized so that the measured epitope map accurately reflects contacts with the protein instead of differences in the T_1 relaxation rates of the ligand protons.[28] Therefore, the effect of saturation time on the extent of STD buildup was measured for a solution of 8 mM (*S*)-propranolol and 0.1 mM AGP with saturation at 0.33 ppm. The results of this experiment are plotted in Figure 7. Although greater dispersion is observed at longer saturation times, the order of the STD effect also changes with saturation time. This can be a problem because it is this ordering of the STD effect that reports on the relative interactions of the ligand protons with the protein. For example, at a saturation time of 0.5 s, $H_{9'}$ has the smallest intensity of the five buildup

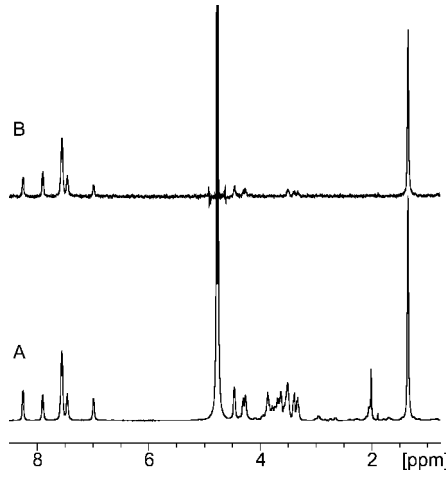

Figure 6. (A) Reference and (B) subtracted (STD) spectra for 2 mM (*R*)-propranolol and 0.1 mM AGP with saturation at 0.33 ppm.

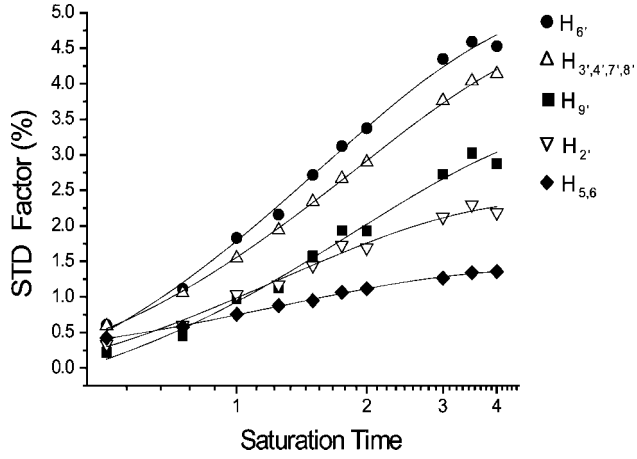

Figure 7. Buildup of STD factor with saturation time, expressed as a percentage.

curves shown; however, at the maximum saturation time, it has the third largest intensity. Although $H_{9'}$ probably does not interact strongly with the protein, as evidenced by our NOESY and diffusion results, the STD effect measured with a 4 s irradiation time appears greater than it should because $H_{9'}$ has the longest T_1 relaxation time of the propranolol naphthyl protons (Supporting Information Table S1). On the basis of these STD buildup curves, a saturation time of 1 s was selected for our experiments. This saturation time is sufficient to provide a good signal-to-noise ratio in the subtracted spectrum while maintaining STD factors that still closely reflect the true ligand−protein interactions by minimizing the effect of differential T_1 relaxation.

The STD epitope maps presented in Table 2 were calculated with on-resonance saturation at 0.33 and 2.6 ppm for several propranolol AGP solutions in which the propranolol is titrated while the AGP concentration remained constant. When on-resonance saturation is centered at 0.33 ppm, the strongest interactions detected in the epitope map are to the hydrophobic methyl and naphthyl protons, with relatively weaker interactions to the naphthyl protons $H_{2'}$ and $H_{9'}$. The largest difference observed between the enantiomers is for the methyl protons, which show a much stronger contact with the protein for the weaker binding (*R*)-propranolol. Although hydrophobic interactions are important, they are fairly nonspecific and probably do not distinguish the binding affinities of the two enantiomers. Saturation at 2.6 ppm for the 2 mM proproanolol and 0.1 mM

TABLE 2: STD Epitope Maps for (*R*)- and (*S*)-Propranolol (Values Are Expressed As a Percentage of the Most Intense Resonance for Each Resonance Integral)

	(*S*)-propranolol:AGP (%)			(*R*)-propranolol:AGP (%)		
	2 mM	4 mM	6 mM	2 mM	4 mM	6 mM
Saturation at 0.33 ppm						
methyl (H_5, H_6)	55	43	38	89	92	80
H_1	32	28	24	38	34	40
H_2	19	25	15	29	19	33
H_3	39	24	15	32	24	34
H_4	19	11	10	21	14	22
$H_{2'}$	58	56	54	55	62	55
$H_{3',4',7',8'}$	90	81	87	97	100	95
$H_{6'}$	100	100	100	100	99	100
$H_{9'}$	62	58	58	66	66	72
Saturation at 2.6 ppm						
methyl (H_5, H_6)	27	21	17	18	19	18
H_1	57	49	45	50	39	37
H_2	46	52	39	39	30	22
H_3	89	70	58	58	58	53
H_4	100	100	100	100	100	100
$H_{2'}$	85	47	40	48	60	50
$H_{3',4',7',8'}$	86	64	56	60	67	59
$H_{6'}$	85	59	44	58	72	60
$H_{9'}$	57	44	29	49	49	50

AGP solution results in much greater saturation for the (*S*)-propranolol H_3 than for the *R* enantiomer. Because this proton is adjacent to both the positively charged amino group and the chiral center, this interaction may reflect different orientations of the two enantiomers with respect to the AGP hydrophilic patch. Although the difference for the H_2 resonance is not as pronounced, a higher level of saturation is again detected for the (*S*)-enantiomer.

Concentration-Dependent Changes in the STD Spectrum. STD experiments for epitope mapping are often measured for very high ligand concentrations, to maximize signal-to-noise ratios.[27,29] However, high ligand concentrations can enhance the contribution of weak nonspecific binding to the measured epitope maps, thwarting attempts to map specific protein interactions onto the ligand.[22] STD experiments have been very successful in mapping the interactions between proteins and hydrophilic sugars where nonspecific binding is less of an issue.[27,30,35] However, STD is also used to map interactions between proteins and small molecule drugs similar to the example investigated in this work. In pharmaceutical applications, the ligand molecules tend to be more hydrophobic and therefore the apparent binding constants for nonspecific binding will be larger and the contribution from nonspecific binding is likely to be of greater concern. Therefore, experiments were also performed to examine the effect of the ligand concentration on the STD results. The STD spectrum measured for a solution of 1 mM (*S*)-propranolol and 0.1 mM AGP had a poor signal-to-noise ratio compared with the subtracted spectrum, even though the total experiment time was increased by a factor of 4 in an attempt to use signal averaging to compensate for the lower ligand concentration. At the magnetic field and AGP concentration used in these experiments, we determined that a propranolol concentration of 2 mM was the smallest that could be used to produce spectra with adequate signal-to-noise ratios for a reasonable investment of instrument time, about 3 h.

For the STD epitope maps calculated with saturation at 0.33 ppm, the only protons showing significant and consistent changes with increasing concentration are (*S*)-propranolol $H_{5,6}$ and H_3. Higher ligand concentrations favor weaker and generally

less specific binding modes involving protein contact with the naphthyl moiety, a privileged protein binding moiety that binds to many proteins in a nonspecific manner.[36] Since eptitope maps are calculated on a relative basis, the concentration-dependent decreases observed for (*S*)-propranolol $H_{5,6}$ and H_3 may reflect a smaller relative contribution from the specific binding mode in which protons near the amine are affected by saturation transfer, compared with nonspecific interactions that inflate the STD intensity of the naphthyl protons.

Discussion

Analysis of the NOESY spectra suggests similar binding modes for the propranolol enantiomers, and no features that distinguish the enantiomers can be detected. The primary intermolecular interactions detected with this experiment involve contacts between the hydrophobic naphthyl and methyl protons of the ligand and the AGP aromatic and methyl protons, consistent with the accepted model of a hydrophobic AGP binding pocket. However, the propranolol naphthyl protons closest to the ether linkage, $H_{2'}$ and $H_{9'}$, show only weak intermolecular NOE cross peaks, and therefore appear to be largely protected from interactions with hydrophobic AGP residues.

In contrast to the NOESY data which reported primarily on hydrophobic interactions, the diffusion data provide strong evidence for an interaction between the charged amino group of propranolol and AGP. However, because the amount of curvature in the diffusion plots is small and because there is not much difference between the various propranolol resonances, it is difficult to confidently extract trends from the data about differences in the binding modes of the two enantiomers. The data for (*R*)-propranolol suggest that $H_{9'}$ is more shielded from the protein than the other protons of the naphthyl ring and there are some differences around the chiral center that may reflect different molecular orientations of the propranolol enantiomers within the binding pocket. The percentage calculated for (*R*)-propranolol H_1 (the chiral center) is somewhat less than that determined for the *S* enantiomer, while the H_3 protons of the *R* enantiomer appear to interact more strongly with the protein. However, caution must be used in extrapolating trends from the diffusion data in Table 1, since the differences observed are small and may not be significant.

Fortunately, the STD experiments produced epitope maps that provide unique insights into the interaction of the propranolol enantiomers with the protons of the AGP binding pocket. When on-resonance saturation is centered at 2.6 ppm, the greatest emphasis in the epitope map is on the hydrophilic propranolol protons near the positively charged secondary amine. The STD epitope maps measured for each enantiomer with on-resonance saturation at 2.6 ppm and at all ligand concentrations agree that the greatest interactions between propranolol and AGP are at H_4, the proton closest to the secondary amine. The epitope maps also show relatively weaker interactions for the naphthyl protons $H_{2'}$ and $H_{9'}$, reinforcing the results obtained with saturation at 0.33 ppm. The maps calculated with saturation centered at 2.6 ppm all agree that the proton at the chiral center (H_2) interacts more strongly with AGP in the *S* enantiomer.

Comparison of the NOESY, Diffusion, and STD Epitope Maps Obtained for the Propranolol Enantiomers. The epitope maps obtained for the *R* and *S* enantiomers of propranolol are similar, consistent with the similar binding constants and the generally accepted model of a flexible or accommodating AGP binding pocket.[2,6,9] Compared with other experiments that have been performed to investigate ligand−AGP interactions, including chromatographic separations, circular dichroism, and fluorescence spectroscopy, NMR has the potential to provide unique and specific information about differences in binding based on the orientation of propranolol functional groups relative to the chiral center. The NOESY, diffusion, and STD results all point to the importance of hydrophobic ligand−protein interactions, consistent with the generally accepted model of the AGP binding pocket. Hydrophobic interactions appear to be important for both the propranolol naphthyl and methyl protons, suggesting that the binding pocket has a large hydrophobic surface. All of the experiments performed suggest that proton $H_{9'}$ is shielded from contact with the protein relative to the other naphthyl protons, which seems reasonable given the structure of propranolol. Although no differences were observed in the NOESY spectra of the two enantiomers, significant differences were detected in the STD epitope maps. Because STD provided better suppression of the protein background than could be achieved in the diffusion experiments, contacts to propranolol H_4 could be detected in the STD spectra. With irradiation at 2.6 ppm, H_4 had the largest STD factor for both enantiomers at all ligand concentrations, reflecting strong interactions between the positively charged secondary amine and the hydrophilic AGP side chains. If the amine group is held relatively firmly near the apex of the AGP binding site, as suggested by previous studies, one would expect to see differences in the epitopes of the propranolol enantiomers, reflecting the different orientation of protons at and around the chiral center. In the STD epitope maps calculated with saturation at 0.33 ppm, the methyl protons $H_{5,6}$ of (*R*)-propranolol appear to contact the protein more closely than for (*S*)-propranolol, while the STD experiment with irradiation at 2.6 ppm shows larger contacts for (*S*)-propranolol H_1, H_2, and H_3. Taken together, the STD results suggest close contacts for H_4 for both enantiomers with stronger hydrophobic interactions for the (*R*)-propranolol methyl protons and for the (*S*)-enantiomer, stronger interactions for the H_1, H_2, and H_3 protons.

There is some disagreement between the epitope maps obtained by STD with irradiation at 2.6 ppm and diffusion in the relative order of for H_1, H_2, and H_3 of (*S*)- and (*R*)-propranolol. The diffusion map suggests closer contacts for (*R*)-propranolol H_3, (*S*)-propranolol H_1, and similar contacts for H_2. These differences may have their origin in inherent differences in the manner in which these experiments are executed, with the STD epitope map resulting from specific irradiation at 2.6 ppm and the diffusion map resulting from nonselective irradiation of all the protein resonances. In addition, the poorer suppression of the protein background in the region of the spectrum containing these resonances introduces greater error in the diffusion results for these protons.

Effect of the Ligand Concentration. All three epitope mapping experiments require that the free and protein-bound ligand are in fast exchange. For binding affinities in the micromolar range, this translates to a ligand concentration in significant excess of the concentration of protein binding sites. Although other researchers suggest the use of a large ligand excess for STD experiments, which translates to large ligand concentrations,[27,29] as the ligand concentration is increased, the epitope map will reflect greater contributions from weaker nonspecific interactions.[37] However, because epitope mapping experiments rely on measurement of ligand resonance intensity, a greater ligand concentration makes it easier to achieve acceptable levels of suppression of the resonances of the protein background. On the basis of these caveats, a ligand concentration for STD experiments must be selected which will balance the

competing factors of signal-to-noise ratio and nonspecific binding contribution to the eptiope map. The ligand concentration for diffusion and NOESY experiments are limited by the nature of the experiments. As the ligand excess is increased, the bound ligand will contribute less to the overall measured signal for diffusion and NOESY epitope mapping experiments.

The primary practical advantage of STD over NOESY and diffusion experiments is the rapid acquisition of data to produce epitope maps. It is possible to acquire an STD epitope map with a propranolol concentration of 1 mM; however, in our hands, this experiment required 12 h and even then produced spectra of considerably poorer quality than those acquired for greater ligand concentrations, so much so that these experiments were not used for epitope mapping. A minimum 2 mM propranolol concentration was required for rapid (3 h) acquisition of STD data for epitope mapping. Therefore, acquisition of a single epitope map at a single ligand concentation with on-resonance saturation centered at a single frequency for each enantiomer required about 6 h of spectrometer time. Additional experiments were required to determine the optimum irradiation time. However, as demonstrated here, drawing conclusions based on an epitope map acquired with on-resonance saturation centered at a single frequency or a single ligand concentration can be misleading, so additional instrument time is required for a more complete analysis. For example, as the ligand concentration is increased, the STD epitope maps for the propranolol enantiomers in Table 2 begin to resemble one another. In the solution containing 2 mM propranolol, the $H_{2'}$ of the *S* enantiomer has a relatively strong STD factor (85%) but a significantly weaker factor (48%) is detected for the *R* enantiomer. However, when the propranolol concentration is increased to 6 mM, $H_{2'}$ shows nearly the same STD factor (within 10%) for both enantiomers. A similar trend is observed for proton H_3. This concentration-dependent behavior can be attributed to increased contributions to the STD effect from nonspecific interactions that do not discriminate between the propranolol enantiomers, reinforcing the assertion that epitope mapping experiments should avoid the use of unnecessarily concentrated ligand solutions regardless of the experiment selected to perform the analysis.

Conclusions

The binding motif derived from these experiments is consistent with the established models of the AGP binding pocket; however, a much greater level of detail about the binding interactions between AGP and the propranolol enantiomers emerges from this study. The positively charged secondary amine of propranolol appears to interact strongly with the patch of negative charge or hydrogen bond donors and acceptors, while the rest of the accommodating/floppy hydrophobic pocket envelopes the naphthyl and methyl groups. The most specific information about preferential interactions of the propranolol enantiomers was obtained from the STD epitope maps which suggested different levels of interaction of the protons of the hydrophilic side chain around the chiral center. However, using multiple experimental approaches to map the interactions between AGP and propranolol adds confidence to the results.

Acknowledgment. B.A.B. acknowledges the support of the National Institutes of Health training grant on Pharmaceutical Aspects of Biotechnology, GM-08359. C.K.L. acknowledges financial support from the American Chemical Society's Petroleum Research Fund grant 42859-AC4 and from NSF CHE-0616811.

Supporting Information Available: Table presenting the T_1 relaxation times measured for a solution containing 8 mM (*R*)- and (*S*)-propranolol and 0.1 mM AGP. This information is available free of charge via the Internet at http://pubs.acs.org.

References and Notes

(1) Nishi, K.; Sakai, N.; Komine, Y.; Maruyama, T.; Halsall, H. B.; Otagiri, M. *Biochim. Biophys. Acta* **2002**, *1601*, 185.
(2) Kaliszan, R.; Nasal, A.; Turowski, M. *Biomed. Chromatogr.* **1995**, *9*, 211.
(3) Lucas, L. H.; Price, K. E.; Larive, C. K. *J. Am. Chem. Soc.* **2004**, *126*, 14258.
(4) Fournier, T.; Medjoubi, N. N.; Porquet, D. *Biochim. Biophys. Acta* **2000**, *1482*, 157.
(5) Hanada, K.; Ohta, T.; Hirai, M.; Arai, M.; Ogata, H. *J. Pharm. Sci.* **2000**, *89*, 751.
(6) Taheri, S.; Cogswell, L. P. III.; Gent, A.; Strichartz, G. R. *J. Pharmacol. Exp. Ther.* **2003**, *304*, 71.
(7) Mao, H.; Hajduk, P. J.; Craig, R.; Bell, R.; Borre, T.; Fesik, S. W. *J. Am. Chem. Soc.* **2001**, *123*, 10429.
(8) Nakagawa, T.; Kishino, S.; Itoh, S.; Sugawara, M.; Miyazaki, K. *Br. J. Clin. Pharmacol.* **2003**, *56*, 664.
(9) Kaliszan, R.; Nasal, A.; Turowski, M. *J. Chromatogr., A* **1996**, *722*, 25.
(10) Xaver de Vries, J.; Schmitz-Kummer, E. *J. Chromatogr., A* **1993**, *644*, 315.
(11) Kopecký, V. Jr.; Rüdiger, E.; Hofbauerová, K.; Baumruk, V. *Biochem. Biophys. Res. Commun.* **2003**, *300*, 41.
(12) Zsila, F.; Iwao, Y. *Biochem. Biophys. Acta* **2007**, *1770*, 797.
(13) Otagiri, M.; Yamamichi, R.; Maruyama, T.; Imai, T.; Suenaga, A.; Imamura, Y.; Kimachi, K. *Pharm. Res.* **1989**, *6*, 156.
(14) Albani, J. R. *Carbohydr. Res.* **2004**, *339*, 607.
(15) Albani, J. R. *Carbohydr. Res.* **2006**, *341*, 2257.
(16) Schmid, K. *J. Am. Chem. Soc.* **1950**, *72*, 2816.
(17) Schmid, K. *J. Am. Chem. Soc.* **1950**, *75*, 60.
(18) Van Dijk, W.; Havenaar, B. C.; Brinkman-van der Linden, E. C. M. *Glycoconjugate J.* **1995**, *12*, 227.
(19) Pellecchia, M. *Chem. Biol.* **2005**, *12*, 961.
(20) Kimura, T.; Shibukawa, A.; Matsuzaki, K. *Pharm. Res.* **2006**, *23*, 1038.
(21) Scherf, T.; Anglister, J. *Biophys. J.* **1993**, *64*, 754.
(22) Lepre, C. A.; Moore, J. M.; Peng, J. W. *Chem. Rev.* **2004**, *104*, 3641.
(23) Lian, L. Y.; Barsukov, I. L.; Sutcliffe, M. J.; Sze, K. H.; Roberts, G. C. K. *Methods Enzymol.* **1994**, *239*, 657.
(24) Utsumi, H.; Seki, H.; Yamaguchi, K.; Tashiro, M. *Anal. Sci.* **2003**, *19*, 1441.
(25) Lucas, L. H.; Yan, J.; Larive, C. K.; Zartler, E. R.; Shapiro, M. J. *Anal. Chem.* **2003**, *75*, 627.
(26) Yan, J.; Kline, A. D.; Mo, H.; Zartler, E. R.; Shapiro, M. J. *J. Am. Chem. Soc.* **2002**, *124*, 9984.
(27) Mayer, M.; Meyer, B. *J. Am. Chem. Soc.* **2001**, *123*, 6108.
(28) Meinecke, R.; Meyer, B. *J. Med. Chem.* **2001**, *44*, 3059.
(29) Yan, J.; Kline, A. D.; Mo, H.; Shapiro, M. J.; Zartler, E. R. *J. Magn. Reson.* **2003**, *163*, 270.
(30) Haselhorst, T.; Weimar, T.; Peters, T. *J. Am. Chem. Soc.* **2001**, *123*, 10705.
(31) Clore, G. M.; Gronenborn, A. M. *J. Magn. Reson.* **1983**, *53*, 423.
(32) Gronenborn, A. M.; Clore, G. M. *Biochem. Pharmacol.* **1990**, *40*, 115.
(33) Ni, F. *Prog. Nucl. Magn. Reson. Spectrosc.* **1994**, *26*, 517.
(34) Derrick, T. S.; McCord, E. F.; Larive, C. K. *J. Magn. Reson.* **2002**, *155*, 217.
(35) Kooistra, O.; Herfurth, L.; Lüneberg, E.; Frosch, M.; Peters, T.; Zähringer, U. *Eur. J. Biochem.* **2002**, *269*, 573.
(36) Hajduk, P. J.; Bures, M.; Praestgaard, J.; Fesik, S. W. *J. Med. Chem.* **2000**, *43*, 3443.
(37) Fielding, L.; Rutherford, S.; Fletcher, D. *Magn. Reson. Chem.* **2005**, *43*, 463.

JP8060366